



Evaluation of the Application of Micromechanical Models in the Estimation of the Modulus of Elasticity for Biocomposites Reinforced with Fique Fiber Braided Ropes

S. Gómez S^{1,2}

¹Dept. Engineering, PhD in Engineering, Universidad Católica Andrés Bello, Caracas, Venezuela.

²Dept. of Mechanical Engineering, Universidad Pontificia Bolivariana, Santander, Colombia.

Received: 09 20 2024; Accepted: 03 05 2025

Available: 12 31 2025

Abstract: This study focuses on the estimation of the longitudinal and transverse moduli of elasticity of biocomposites reinforced with fique fiber in braided-rope configuration and a natural rubber matrix, using semi-empirical micromechanical models. First, both the fique fiber rope and the natural rubber matrix were mechanically characterized. Using the obtained data, the micromechanical models of the Rule of Mixtures, Halpin-Tsai, Chamis, Hopkins & Chamis, Nielsen, Miravete, Jones, and Yung Fu were applied to calculate the corresponding moduli. Subsequently, biocomposites were manufactured with fique fibers oriented at 0° and 90°, with the fiber volume fraction varied. The biocomposites were characterized to determine the longitudinal and transverse moduli. The comparison of results showed that Miravete's and Yun Fu's micromechanical models provided the best fits for these materials.

Keywords: biocomposite, fique, micromechanical models, modulus of elasticity, rule of mixtures.

*Corresponding author.

E-mail address: sergio.gomez@upb.edu.co (S. Gómez).

Peer Review under the responsibility of Universidad Nacional Autónoma de México.

1. Introduction

A composite material is a combination of two different materials to improve their individual mechanical properties. This type of material includes biocomposites or natural composites that incorporate one or more natural components (Hiremath et al., 2024).

Composite modeling plays a fundamental role in predicting the mechanical properties of these materials before they are manufactured. This predictive approach is essential for optimizing the design and ensuring the desired performance in the various industrial applications where they will be used (Wang & Huang, 2017).

This approach encompasses several scales of analysis, beginning with the microscale, which is devoted to the detailed study of constituent elements such as fiber and matrix. It then moves to the mesoscale, which focuses on the laminar configuration or layering of the composite. Finally, the macroscale is examined, where the structure as a whole and its interactions with external forces are analyzed (Raju et al., 2018).

Despite advances, the modeling of composite materials remains a significant challenge to accurately predict their mechanical properties. This is due to the anisotropic and inhomogeneous nature of these materials, together with their multiple failure modes and complex interactions, especially under multiaxial loading conditions (Wan et al., 2023).

In microanalysis of composites, micromechanical models are used. These models use the properties of the constituent materials to determine the composite's macroscopic properties (Wang & Huang, 2018).

Both analytical and numerical methods are available to perform micromechanical analysis. With advances in technology and computing power, there has been an increasing preference for numerical approaches. However, analytical modeling remains important as a first step, especially in contexts where optimization involves a large number of variables (Andrianov et al., 2017).

Analytical models include semi-empirical micromechanical models that combine fundamental physical principles with empirical parameters derived from experimental data. These models use a synthesis between the theoretical foundations of mechanics of materials and experience derived from experimental observations to characterize the behavior of composite materials (Jasti et al., 2023).

There are several semi-empirical micromechanical models for predicting the properties of fiber-reinforced composites (Loos, 2014). One of them is the Rule of

Mixtures (ROM), which is based on the assumption that the individual components of the composite material retain their characteristic properties, such as strength, stiffness, density, etc., and that these properties combine in a weighted manner according to the volume fraction of each component in the composite material (Jagadeesh & Gangi Setti, 2020).

The classical ROM model, known for its mathematical simplicity and predictive accuracy, has evolved by incorporating additional variables, such as fiber length and diameter, orientation, interfacial shear strength, and other relevant parameters. These advances have led to new semi-empirical models based on the rule of mixtures, which offer a significant improvement in the predictive ability and understanding of the behavior of composite materials (Tham et al., 2019).

In the field of engineering, several models based on ROM are used. Among them, the model of Chamis, Halpin, Tsai, Nielson, and the contributions of Hopkins & Chamis stand out (Alhijazi et al., 2021). Each of these models has been fundamental in the analysis and design of structures in various fields of engineering, from predicting the behavior of composite materials to evaluating structural integrity under critical conditions.

Various semi-empirical analytical models are often used to predict the mechanical properties of composite materials reinforced with synthetic fibers (Jasti et al., 2023). However, according to Potluri et al. (2018), their application in predicting such properties in natural fiber reinforced biocomposites is considerably less.

Despite this, studies have applied semi-empirical analytical models to natural fiber-reinforced biocomposite materials. For example, Alhijazi et al. (2021) estimated longitudinal, transverse, and shear moduli for loofah and palm natural fiber biocomposites using epoxy and ecoepoxy matrices, and applied the micromechanical models of the rule of mixtures, Chamis, Halpin-Tsai, and Nielsen. As a result, they found that the Chamis model gave the highest property values, while the Halpin-Tsai model gave the lowest. On the other hand, Gigante et al. (2017) investigated a biocomposite material consisting of a PLA matrix and cellulose fibers, and their results showed that the Halpin-Tsai model provides an accurate estimate of the transverse component of the modulus of elasticity, which agrees well with the experimental values obtained. In addition, Fajardo et al. (2022) reproduced the stress-strain curves of a biocomposite with guadua fiber using the Kelly-Tyson and Isitman-Aykol micromechanical models and obtained low residual standard deviations.

According to Muñoz-Blandon et al. (2023), one of the fibers with high potential for use as a natural reinforcement in biocomposite materials is the fique fiber. This is due to its remarkable holocellulose content and its low lignin and pectin content. These characteristics suggest that fique fiber may be a promising option for improving the properties of composite materials in various industrial applications.

Research on micromechanical models applied to fiber-reinforced composites is scarce in the literature. An outstanding study is that of González-Estrada et al. (2018), who used the rule of mixtures model to analyze the longitudinal modulus of elasticity in biocomposites containing 2, 3, and 4 fique fibers (it is important to note that no information was provided on the volume or weight fraction of the fibers). This study compared the results with experimental data and showed a maximum error of 5.06%. Despite these results, the study was limited to the mixing rule model, without exploring other available micromechanical models or performing analyses to estimate the transverse modulus of elasticity or other mechanical properties of the biocomposite material.

This research limitation underscores the imperative need for future studies that address a wider range of micromechanical models, as well as additional analyses to deepen the understanding of the mechanical behavior of fique-fiber-reinforced biocomposites. As noted by Vignoli et al. (2019), despite previous studies on analytical micromechanical models, a considerable lack of understanding persists regarding their estimation, especially regarding transverse elastic properties and strengths.

In addition, the literature has focused on the application of micromechanical models to synthetic fibers, which are treated as individual long fibers due to the standard manufacturing process (Bunsell & Renard, 2005; Sudheer et al., 2015), but there is a paucity of information on research conducted on braided ropes. This lack of studies is significant as fique is often marketed in the form of braided ropes by artisanal communities. Therefore, it is crucial to explore the applications of this fiber in such a configuration to take advantage of what the market offers, while evaluating the applicability of micromechanical models in this type of fiber arrangement.

On the other hand, only one study by Velásquez et al. (2018) stands out, in which rubber is used as a matrix for the manufacture of a composite material reinforced with fique fibers. This research focused on the experimental characterization of the mechanical properties and resistance to abrasive wear. According to the authors, this composite material has potential for commercial

applications, which highlights the need for further research with this type of natural matrix.

For this reason, in this study, the estimation of the longitudinal and transverse moduli of elasticity of biocomposite materials reinforced with different proportions of fique fibers in a braided rope configuration and natural rubber matrix is performed. This estimation is performed by evaluating different micromechanical models, including the Rule of Mixtures, Halpin-Tsai, Chamis, Hopkins & Chamis, Nielsen, Miravete, Jones, and Yung Fu. The results from these models are compared with the experimental data to determine which provides the highest accuracy.

This study is particularly relevant for the development of sustainable composite materials. Given that fique fiber is a renewable natural resource, its use as reinforcement reduces dependence on synthetic materials and promotes eco-friendly alternatives. Accurately evaluating and predicting its modulus of elasticity is essential for optimizing its mechanical performance in technical applications. Moreover, comparing different micromechanical models improves the precision with which these materials are characterized. These biocomposites have potential applications in sectors such as the automotive industry, for the manufacturing of lightweight and durable components, and in construction, for insulation systems and vibration dampers (Agudelo et al., 2024; Laverde et al., 2025)

2. Materials and Methods

2.1 Materials

For the fabrication of the biocomposites, braided fique fiber was selected, consisting of multiple intertwined fibers forming a single filament. This choice was based on its commercial availability in this configuration within the local market. The fibers were supplied by Ecofibras, a company located in Curití, Santander, Colombia.

To achieve a more uniform distribution within the matrix, the smallest-diameter commercially available fique rope, with a density of 810 kg/m^3 , was selected. It had an average diameter of $1.94 \pm 0.075 \text{ mm}$, as shown in Figure 1, obtained using a Tescan MIRA 3 FEG-SEM scanning electron microscope. The micrograph, captured at 100X magnification, provided a detailed view of the fiber structure.

In relation to the matrix of the composite, it was decided to use natural rubber, which has a density of 917 kg/m^3 , obtained from the centrifugation of natural latex and preserved with an ammonia level of 0.60% w/w. The natural rubber was supplied by Panamericana, a company located in Bucaramanga, Santander, Colombia.

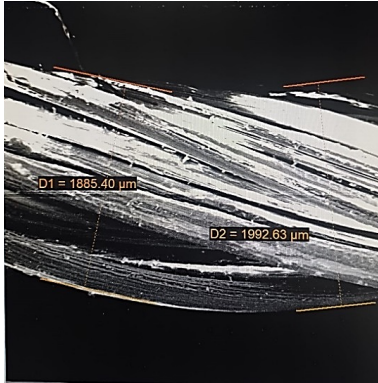


Figure 1. SEM image of the braided fique rope.

2.2 Fiber and Matrix Mechanical Characterization

Tensile tests were used to evaluate both the natural fiber rope and the matrix using an MTS Universal Tester, Model C43.104, with a maximum capacity of 10 KN. These tests were conducted at a controlled temperature of $23.1^{\circ}\text{C} \pm 3^{\circ}\text{C}$ to ensure consistency of results.

Tensile testing of the fibers in rope configuration was performed in accordance with ASTM C1557-20, "Standard Test Method for Tensile Strength and Young's Modulus of Fibers". Five specimens, each $150\text{ mm} \pm 0.3\text{ mm}$ in length, were prepared and tested at a constant rate of 0.48 mm/min in accordance with established regulatory requirements. Figure 2 shows the experimental procedure used.

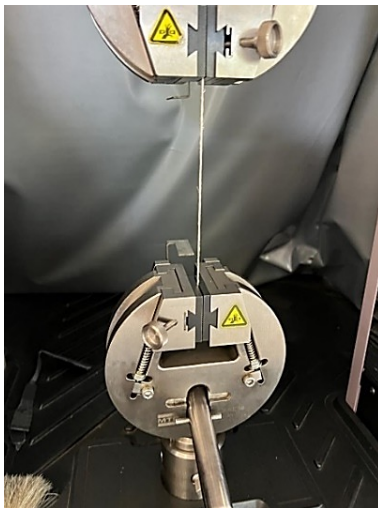


Figure 2. Tensile test of fique braided rope.

For natural rubber, tests were performed in accordance with ASTM D412-16, "Standard test methods for vulcanized rubber and thermoplastic elastomers – Tension".

These tests were carried out at a speed of 500 mm/min using five specimens, each $3.2\text{ mm} \pm 0.4\text{ mm}$ thick, in accordance with the standard's specified dimensions. The specimens had a width of $25\text{ mm} \pm 0.1\text{ mm}$ and a length of $115\text{ mm} \pm 2.1\text{ mm}$ according to method A (dumbbell and straight specimens), type C specified in the standard. The specimens made with the natural rubber material are shown in Figure 3.

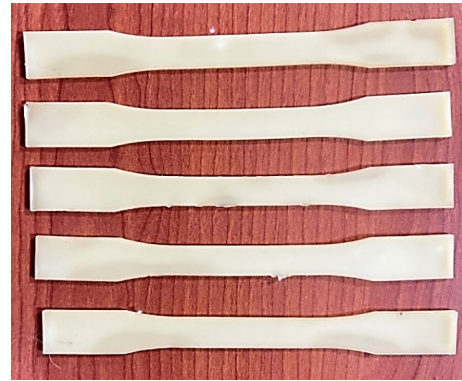


Figure 3. Natural rubber tensile test specimens.

Both the fiber and the natural rubber matrix are considered to be isotropic materials, meaning that they have a uniform modulus of elasticity in both the longitudinal and transverse directions. Therefore, a single value is used in the corresponding equations.

2.3 Biocomposites Fabrication and Characterization

To produce the biocomposites, the fibers were arranged on a flat mold that had previously been treated with a release agent, according to the required volume of fique fibers (number of fiber filaments) and the desired fiber orientation. Natural rubber was then uniformly applied to the fibers. The material was cured at room temperature for 3 days, followed by an 8-hour treatment in a forced-convection oven at 35°C .

The mechanical properties of the composites were analyzed by tensile testing in accordance with ASTM D3039/D3039M-17, "Standard Test Method for Tensile Properties of Polymer Matrix Composite Materials". This test was performed at an ambient temperature of $22.8^{\circ}\text{C} \pm 2.2^{\circ}\text{C}$ and a constant speed of 2 mm/min using the MTS Universal Testing Machine, Model C43.104.

Specimens were prepared with fibers oriented at two different angles, 0° and 90° , indicating the orientation of the fibers with respect to the force applied by the universal machine. This was done to estimate the longitudinal and transverse moduli.

The specimens oriented at 90° (for the evaluation of the transverse modulus) had a constant thickness of 2 mm ± 0.4 mm and dimensions of 25 mm ± 1.6 mm in width and 175 mm ± 2.1 mm in length, in accordance with the normative guidelines. Seven biocomposite materials were tested, each with a different volumetric fraction of fique fiber: 2.4%, 4.8%, 7.8%, 8.5%, 13%, 16%, and 24%. These fractions correspond to 10, 20, 40, 40, 60, 60, 80, 100, and 120 braided fique fiber ropes, all arranged transversely. Figure 4 illustrates the fabricated transverse braided fiber biocomposites.



Figure 4. Transverse braided fiber biocomposites.

On the other hand, the specimens oriented at 0° (for the evaluation of the longitudinal modulus) had a uniform thickness of 1 mm ± 0.3 mm and dimensions of 15 mm ± 1.3 mm in width and 250 mm ± 3.4 mm in length, in accordance with regulatory guidelines. Five specimens were prepared for each volumetric fraction of fique fiber (5%, 8%, 15%, 17%, 23%, and 25%), corresponding to 3, 6, 9, 12, 15, and 18 braided fique fiber ropes, all aligned in the longitudinal direction. Figure 5 illustrates the fabricated longitudinally braided fiber biocomposites.

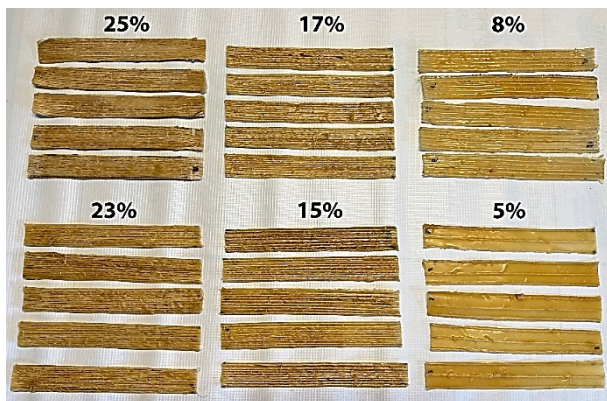


Figure 5. Longitudinally braided fiber biocomposites.

Figure 6 illustrates the tensile test and provides a clear visual representation of the experimental process.



Figure 6. Tensile testing of biocomposites.

2.4 Micromechanical Models

Micromechanical models based on the Rule of Mixtures were used to analytically calculate the modulus of elasticity and compare it with experimental results. Specifically, the Rule of Mixtures, Halpin-Tsai, Chamis, Hopkins & Chamis, Nielsen, Miravete, Jones, and Yung Fu models were selected and applied.

The selection of these models was based on their application in predicting the mechanical properties of composite materials. The Rule of Mixtures (ROM) provides an initial estimate that does not account for fiber-matrix interactions (Jasti et al., 2023). Halpin-Tsai adjusts the fiber contribution using a geometric factor, while Nielsen incorporates porosity and maximum volume fraction, enhancing accuracy for biocomposites with irregular reinforcement (Alhijazi et al., 2021). Chamis introduces a correction based on fiber volume fraction, and Hopkins & Chamis refine this approach by adjusting the matrix contribution (Raju et al., 2018). Miravete considers matrix anisotropy and its interaction with the fiber, which is crucial for composites with flexible matrices, such as natural rubber (Miravete, 2020). Jones employs reciprocal averaging to improve the estimation of transverse stiffness (Hajikarimi & Sadat Hosseini, 2023) and matrix all around the fibers. The 2-axis is perpendicular to 1-axis in the lamina plane and 3-axis is normal to this plane. The 1–2–3 system is the local coordinate system of an anisotropic material which is required to be defined when mechanical

properties of a lamina are formulated. All the formulations presented here are in the lamina local coordinate system unless it is stated that the global coordinate system (x–y–z system, while Yun Fu incorporates empirical adjustments to optimize its application in natural fiber biocomposites (Fu et al., 1998).

To determine the longitudinal elastic modulus of the fibers, all selected micromechanical models use the same mathematical equation derived from the Rule of Mixtures. Given that these models assume a uniform stress distribution in which the fibers primarily bear the load, they do not introduce variations in the predicted values in this direction. Therefore, Equation 1 represents the longitudinal modulus of all models (Alhijazi et al., 2021).

$$E_1 = E_f * V_f + E_m * (1 - V_f) \tag{1}$$

Where E_f represents the modulus of elasticity of the fiber, V_f denotes the volume fraction of the fiber, and E_m is the modulus of elasticity of the matrix.

The following equations were used to determine the transverse modulus of elasticity for each micromechanical model.

- Rule of Mixtures: Also known as the inverse rule of mixtures (IROM), where the modulus of elasticity is defined according to Equation 2 (Alhijazi et al., 2021; Efendy & Pickering, 2019; Jagadeesh & Gangi Setti, 2020; Jasti et al., 2023; Vignoli et al., 2019).

$$E_2 = \frac{E_f * E_m}{E_m * V_f + E_f * (1 - V_f)} \tag{2}$$

- Halpin Tsai. The transverse modulus of elasticity used in the Halpin-Tsai model is defined according to Equations 3 and 4 (Alhijazi et al., 2021; Efendy & Pickering, 2019; Jasti et al., 2023; Sudheer et al., 2015; Vignoli et al., 2019).

$$E_2 = E_m \left(\frac{1 + \zeta * \eta * V_f}{1 - \eta * V_f} \right) \tag{3}$$

where

$$\eta = \left(\frac{\frac{E_f}{E_m} - 1}{\frac{E_f}{E_m} + \zeta} \right) \tag{4}$$

ζ is a geometric parameter that represents the geometry of the reinforcement, the packing geometry and the loading conditions, as expressed in Equation 5.

$$\zeta = 2 \frac{l}{d} \tag{5}$$

Where l is the length of the fibers in the composite and d is the fiber diameter or particle size. Taking into account that the fibers are cylindrical and are arranged in a square arrangement, its value can be assumed to be as expressed by Equation 6 (Efendy & Pickering, 2019).

$$\zeta = 2 \tag{6}$$

- Chamis: The transverse modulus of elasticity in the Chamis model is determined by Equation 7 (Alhijazi et al., 2021; Raju et al., 2018; Sudheer et al., 2015; Vignoli et al., 2019; Wang & Huang, 2017).

$$E_2 = \frac{E_m}{1 - (\sqrt{V_f} * (1 - \frac{E_m}{E_f}))} \tag{7}$$

- Hopkins & Chamis: The transverse modulus of elasticity used in the Hopkins & Chamis model is defined by Equation 8 (Bunsell & Renard, 2005; Raju et al., 2018).

$$E_2 = E_m \left[(1 - \sqrt{V_f}) + \frac{\sqrt{V_f}}{1 - \sqrt{V_f} * (1 - \frac{E_m}{E_f})} \right] \tag{8}$$

- Nielsen: The transverse modulus of elasticity in the Nielsen model is defined according to Equations 9, 10, and 11 (Alhijazi et al., 2021; Efendy & Pickering, 2019; Sudheer et al., 2015).

$$E_2 = E_m \left(\frac{1 + \zeta * n * V_f}{1 - \psi * n * V_f} \right) \tag{9}$$

Where

$$n = \left(\frac{\frac{E_f}{E_m} - 1}{\frac{E_f}{E_m} + \zeta} \right) \tag{10}$$

And

$$\psi = 1 + \frac{(1 - \psi_{max})}{\psi_{max}^2} * V_f \tag{11}$$

It is established that, in a square fiber arrangement, the maximum value of ψ is 0.785. Since the model considers the arrangement of cylindrical fibers in a square formation, $\zeta = 2$ is set as a predefined parameter (Alhijazi et al., 2021; Efendy & Pickering, 2019).

- Miravete: The transverse modulus of elasticity described by Miravete is defined according to Equation 12 (Miravete, 2020).

$$E_2 = \frac{E_m}{(1 - v_m^2)^{1.25} * (1 + 0.85 v_f^2)} * \frac{E_m * V_f}{(1 - V_f)^{1.25} + \frac{E_f * V_f}{1 - v_m^2}} \tag{12}$$

v_m is defined as Poisson's coefficient of the matrix

- Jones: The transverse modulus of elasticity used in the Jones model is defined by Equation 13 (Hajikarimi & Sadat Hosseini, 2023).

$$\frac{1}{E_2} = \frac{1}{V_f + 0.5 * (1 - V_f)} * \left(\frac{V_f}{E_f} + 0.5 * \frac{(1 - V_f)}{E_m} \right) \tag{13}$$

- Yun Fu: The transverse modulus of elasticity used in Yun Fu's model is defined according to Equation 14 (Fu et al., 1998; Raju et al., 2018).

$$\frac{1}{E_2} = \frac{\sqrt{\frac{4V_f}{\pi}}}{\sqrt{\frac{\pi V_f}{4} * E_f + \left(1 - \sqrt{\frac{\pi V_f}{4}}\right) * E_m}} + \frac{\left(1 - \sqrt{\frac{4V_f}{\pi}}\right)}{E_m} \quad (14)$$

It is crucial to emphasize that for the effective application of micromechanical models, it is necessary to know the fiber volume fraction present in the biocomposites. However, from an experimental standpoint, it is more feasible to measure the fiber fraction. Therefore, Equation 15 was used to calculate the volume fraction of fiber required by the models (Efendy & Pickering, 2019; Bunsell & Renard, 2005)

$$V_f = W_f * \frac{\rho_c}{\rho_f} \quad (15)$$

Where ρ_f is the density of the fiber, ρ_c is the density of the composite, and W_f is the fiber weight fraction calculated according to Equation 16.

$$W_f = \frac{w_f}{w_c} \quad (16)$$

Where w_f is the weight of the fiber and w_c is the weight of the composite.

2.5 Statistical Analysis

In order to determine whether the results of tensile stress and elastic modulus of the composite biomaterials showed statistically significant differences depending on the different amounts of fibers, the ANOVA (Analysis of Variance) technique was used. If the p-value (Probability) is less than the established significance level (0.05), it is concluded that at least one of the mean values of the mechanical properties is significantly different.

To analyze the differences between the average modulus of elasticity obtained experimentally and the predictions of the micromechanical models, the percentage error was calculated using Equation 17.

$$\%E = \frac{|X-Y|}{Y} * 100 \quad (17)$$

Where X is the value obtained from the different micro-mechanical models and Y is the average value obtained from the experimental results.

3. Results

3.1 Mechanical Characterization of the Fiber and the Matrix

The stress-strain curve resulting from the tensile test performed on the natural fique fiber rope is shown in Figure 7. Initially, the fiber rope exhibits a linear behavior where

the stress and strain maintain a direct proportional relationship until the breaking point is reached. However, when the maximum stress is reached, the material does not break abruptly, as would be expected for brittle materials. This is due to the fact that the rope is composed of multiple braided fique fibers, which allows some fibers to break first while the remaining fibers continue to support the load. This behavior gives the material greater toughness and distributes the load more gradually until the rope breaks completely.

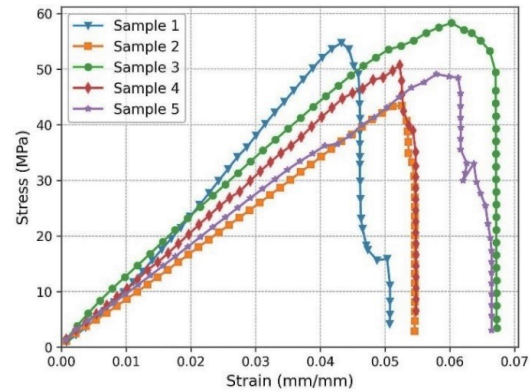


Figure 7. Strain-stress curve of braided fique rope.

The maximum tensile stress recorded was 51.90 ± 5.1 MPa, while the modulus of elasticity reached 1.12 ± 0.225 GPa. The tensile stress obtained is in agreement with the values reported by Gómez-Suarez & Córdoba-Tuta (2022) in their review of composite materials made with fique fiber, where it is established that this stress varies between 43 and 571 MPa for a single fique fiber. However, it is important to note that the observed modulus of elasticity is lower than that reported in the literature, which ranges from 8.2 to 9.1 GPa for single unbraided fique fibers. This discrepancy in the modulus of elasticity can be attributed to the braided structure of the rope, where not all fibers are perfectly aligned with the direction of the applied load, reducing the overall stiffness of the material. In addition, interactions between the braided fibers, such as friction and slippage, contribute to the increased flexibility of the rope.

Figure 8 shows the stress-strain curve of natural rubber. The curve begins with an elastic region where the material responds linearly to applied stress, showing a directly proportional relationship between stress and strain. This behavior is maintained until the material reaches its elastic limit. At this point, the rubber enters a region of non-linear deformation, where large

deformations occur for relatively small increments of stress. Finally, as the stress continues to increase, the rubber enters the hardening zone, where the curve rises more steeply. This is because the molecular chains of the rubber are fully stretched and aligned in the direction of the stress, showing increased resistance to further deformation.

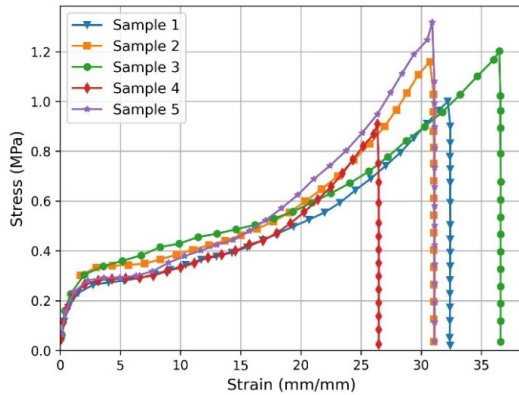


Figure 8. Stress-strain curve natural rubber.

In the test, the maximum tensile stress recorded for natural rubber was 1.14 ± 0.16 MPa, with a modulus of elasticity of 0.299 ± 0.023 MPa. Additionally, Poisson’s coefficient obtained was 0.51 ± 0.11 .

3.2 Mechanical Properties of Biocomposites

The mechanical properties of the biocomposites obtained with braided fique fiber arranged longitudinally in different volume fractions, including the maximum tensile stress and modulus of elasticity, are shown in Figures 9 and 10, respectively.

Both the mechanical strength and the elasticity modulus of the biocomposite materials with longitudinal fibers increase as the percentage of Fique fibers increases. This behavior is due to the fact that the fique fibers reinforce the matrix, distributing the stresses more uniformly and improving the material’s ability to absorb and dissipate energy. In addition, since the fibers have an intrinsic strength greater than that of the matrix, they contribute significantly to the higher load-bearing capacity of the material.

The biocomposite with the highest fiber volume fraction of 25% showed the best mechanical performance, reaching a maximum stress of 19.11 ± 0.79 MPa and a modulus of elasticity 277.24 ± 17.48 MPa. These results highlight the positive influence of the fiber on the mechanical properties of the material.

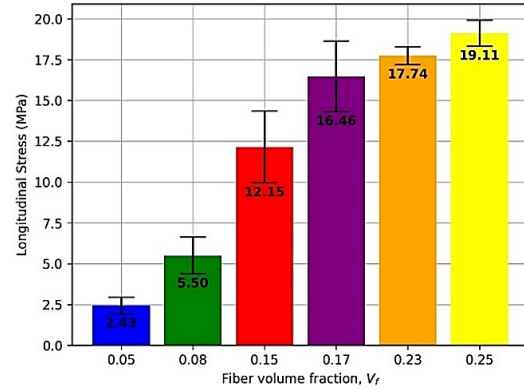


Figure 9. Tensile stress, biocomposites with longitudinal braided fibers.

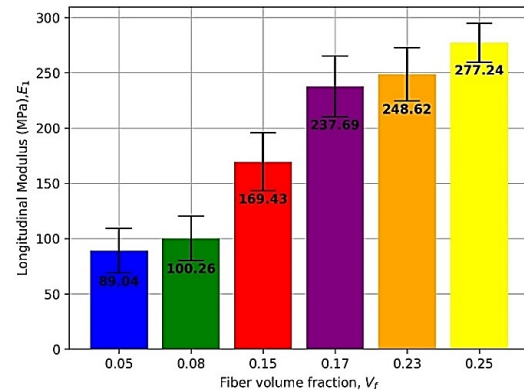


Figure 10. Elastic modulus of biocomposites with longitudinal braided fibers.

The maximum tensile stress, modulus of elasticity of the composite biomaterials prepared with braided fique fibers arranged transversely at different fiber volume fractions are shown in Figures 11 and 12, respectively.

When evaluating the behavior of biocomposite materials made with transverse fibers, it is observed that the modulus of elasticity reaches a maximum of $1.08 \text{ MPa} \pm 0.084 \text{ MPa}$ in the biocomposite with 24% fiber volume. This behavior is comparable to that of composites with longitudinal fibers, where higher fiber content also increases the modulus. However, in terms of tensile stress, the results show similar values for the different fiber volume fraction percentages, ranging from 0.11 MPa to 0.15 MPa. This is because the fibers arranged transverse to the principal load do not contribute significantly to the tensile strength in that direction. As a result, the composite does not fully leverage the fibers’ mechanical properties to support the load in the desired direction, leading to increased loading in the matrix.

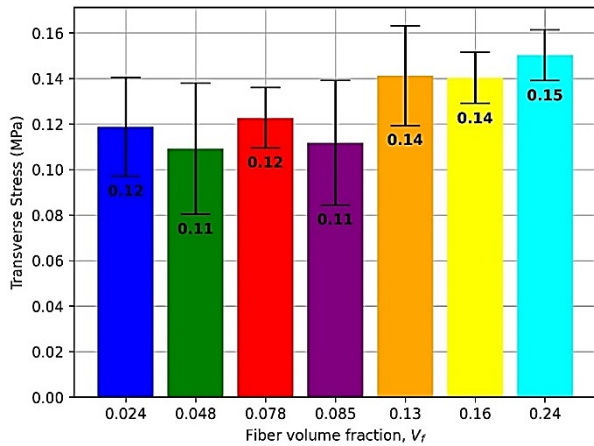


Figure 11. Tensile stress, biocomposites with transverse braided fibers.

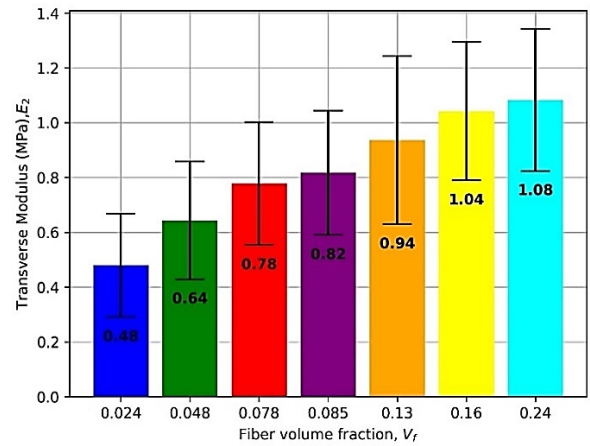


Figure 12. Elastic modulus, biocomposites with transverse braided fibers.

The results of the ANOVA test are presented in Table 1. These results indicate that both the tensile stress and modulus of elasticity of the biocomposites with longitudinally arranged braided fique fiber and with different fiber volumes have p-values less than 0.05. This suggests that at least one of the biocomposites presents a significantly different mean compared to the others. In contrast, for the biomaterials with braided fique fiber arranged transversely, the results show that, in tensile stress, a

p-value of 0.05 was obtained, indicating that there are no statistically significant differences in the means of the biocomposites. However, for the modulus of elasticity, the p-value was less than 0.05, suggesting that at least one of the means is significantly different from the others.

When comparing the maximum tensile stress and modulus of elasticity of materials with longitudinally and transversely oriented fibers, a significant advantage is observed for those with longitudinally oriented fibers.

Table 1. ANOVA test.

Property	Source	Sum of squares	Degree of freedom	Mean square	Fo	P
Longitudinal tensile stress	Biocomposites	1184.86	5	236.97	95.90	<0.001
	Residuals	59.30	24	2.470		
	Total	1244.16	29			
Longitudinal elasticity modulus	Biocomposites	159689.24	5	31937.84	48.80	<0.001
	Residuals	15705.60	24	654.40		
	Total	175394.85	29			
Transverse tensile stress	Biocomposites	0.00776	6	0.00129	2.46	0.005
	Residuals	0.014756	28	0.00052		
	Total	0.02252	34			
Transverse elasticity modulus	Biocomposites	1.401	6	0.233	3.212	0.016
	Residuals	2.036	28	0.072		
	Total	3.437	34			

This superiority is due to the fact that the fibers in this orientation are better positioned to support and distribute the load efficiently, thus maximizing their intrinsic strength. The longitudinal orientation also promotes more effective load transfer between the matrix and the fibers, thereby improving the material's internal cohesion. In contrast, transversely oriented fibers cannot take full advantage of their strength due to their perpendicular orientation to the load, resulting in a reduced ability to withstand high stresses.

3.3 Micromechanical Model Evaluation

Figure 13 shows the longitudinal elastic modulus as a function of the fiber volume fraction, calculated using all the selected micromechanical models, which employ the same equation in the longitudinal direction, along with the values obtained from the experimental tests. This is because these models assume a uniform stress distribution, where the fibers primarily bear the load.

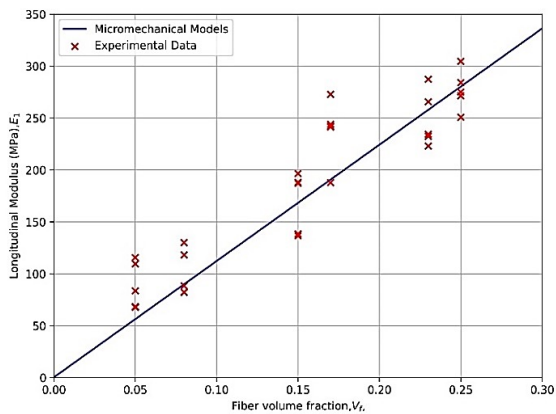


Figure 13. Longitudinal modulus of elasticity predicted by the micromechanical models.

It is observed that the models show an increase in the longitudinal modulus of elasticity with increasing fiber volume fraction, a trend that is consistent with the results obtained in the experimental tests.

Table 2 shows the percentage error as a function of the longitudinal fiber volume fraction, comparing the results of the micromechanical models with the average of the experimental results.

The data show that the percentage error varies significantly as a function of fiber volume fraction. As the fiber fraction increases, the percent error fluctuates significantly, with a maximum of 36.9% in the biocomposite with 5% fiber volume fraction and a minimum of 0.7% in the biocomposite with 15% fiber volume fraction.

Table 2. Percentage error in longitudinal modulus of elasticity.

Fiber volume fraction Vf (%)	% E
5	36.9
8	10.4
15	0.7
17	19.8
23	3.7
25	1.1

Figure 14 shows the transverse modulus of elasticity as a function of fiber volume, as estimated by the various micromechanical models.

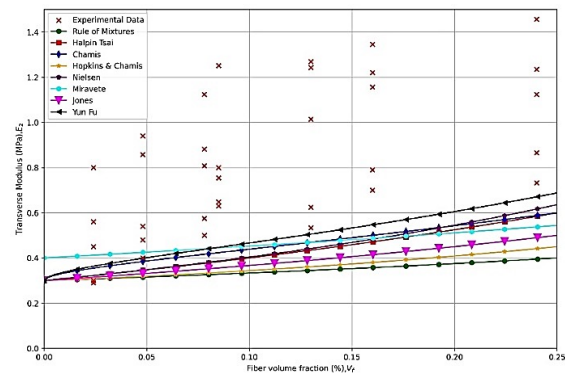


Figure 14. Transverse modulus of elasticity predicted by the micromodels.

It is observed that the Yun Fu model predicts higher values for higher volume fractions, while the model based on the Rule of Mixtures gives the lowest predictions. All micromechanical models show an increase in the modulus of elasticity with increasing fiber content, following the trend observed in the experimental data. However, the experimental results exceed the model predictions.

Table 3 presents the percentage error as a function of the transverse fiber volume fraction, comparing the results of the different micromechanical models with the average experimental results.

The results show significant variability in percentage error between models and as a function of fiber fraction. In general, the Rule of Mixtures model has the highest percentage error across all volume fractions. In contrast, the Halpin-Tsai and Chamis models have relatively smaller but still significant errors. The Miravete model offers lower errors compared to the others, especially in fiber fractions below 7.8%. Yun Fu's model shows the lowest errors for fiber fractions above this percentage.

Table 3. Percentage error in transverse modulus of elasticity.

Fiber volume fraction Vf (%)	% E							
	Rule of Mixtures	Halpin- Tsai	Chamis	Hopkins & Chamis	Nielsen	Miravete	Jones	Yun Fu
2.4	35.96	32.89	26.05	35.73	32.85	14.14	34.43	24.29
4.8	50.76	46.04	39.98	50.24	45.91	33.67	48.40	37.76
7.8	58.29	51.79	46.64	57.38	51.49	43.53	55.03	43.87
8.5	60.02	53.23	48.36	59.03	52.89	45.83	56.62	45.51
13	63.32	53.79	50.10	61.60	53.03	50.08	58.55	46.23
16	65.66	54.69	51.93	63.46	53.57	53.19	60.17	47.46
24	63.45	45.93	45.56	59.16	42.94	50.25	54.69	37.93

These errors are consistent with existing literature. According to Efendy & Pickering. (2019), a discrepancy of up to 140% has been observed when micromechanical models are used to predict the modulus of elasticity of natural fiber composites. As an example, in their research on composites reinforced with natural harakeke and hemp fibers, they found that models such as the Rule of Mixtures tend to underestimate the modulus of elasticity, with errors of up to 71% for harakeke and up to 120% for hemp. These results highlight the inherent limitations of micromechanical models in accurately predicting the mechanical properties of natural fiber composites, primarily due to the heterogeneity and variability of these fibers. In this context, the errors obtained in this study fall within an expected range, consistent with the capability of micromechanical models for these materials.

Conclusions

This study assessed the effectiveness of various micromechanical models in estimating the longitudinal and transverse moduli of elasticity in biocomposites reinforced with braided fique-fiber ropes and a natural rubber matrix. The results highlight the significant influence of fiber orientation on the mechanical properties of the composites. Longitudinally aligned fibers contributed to higher tensile strength and modulus of elasticity, whereas transversely oriented fibers had a limited impact on tensile strength due to their perpendicular arrangement to the applied load.

Regarding the micromechanical modeling of the longitudinal elastic modulus, models using the same equation based on the Rule of Mixtures provided reasonable estimates. However, the percentage error varied significantly

as a function of fiber volume fraction. These results indicate that although the rule of mixtures is a useful tool, its predictive accuracy is highly dependent on the composition of the biocomposite.

For the prediction of transverse modulus, Miravete's model presented the lowest errors at reduced fiber fractions, while Yun Fu's model showed higher accuracy at higher fiber fractions. However, all of these micromechanical models tended to underestimate the transverse modulus, suggesting that they may not fully capture the mechanical behavior of natural fibers braided within a rubber matrix.

Conflict of interest

The author has no conflict of interest to declare.

Funding

The author received no specific funding for this work.

References

- Agudelo, L. R. A., de Freitas, L. F. F., Velasco, D. C. R., Vieira, C. M. F., L, H. a. C., & Lopez, F. P. D. (2024). Caracterização da fibra como reforço sustentável para compósitos de polímero. *ABM Proceedings*, 2541–2550. <https://doi.org/10.5151/2594-5327-41251>
- Alhijazi, M., Safaei, B., Zeeshan, Q., & Asmael, M. (2021). Modeling and simulation of the elastic properties of natural fiber-reinforced thermosets. *Polymer Composites*, 42(7), 3508–3517. <https://doi.org/10.1002/pc.26075>

- Andrianov, I. V., Awrejcewicz, J., & Danishevskyy, V. V. (2017). Models of Composite Materials and Mathematical Methods of Their Investigation. In *Asymptotical Mechanics of Composites: Modelling Composites without FEM* (pp. 21-67). Cham: Springer International Publishing.
https://doi.org/10.1007/978-3-319-65786-8_2
- Bunsell, A. R., & Renard, J. (2005). Fundamentals of Fibre Reinforced Composite Materials.
<https://doi.org/10.1201/9781420056969>
- Efendy, M. A., & Pickering, K. L. (2019). Comparison of strength and Young modulus of aligned discontinuous fibre PLA composites obtained experimentally and from theoretical prediction models. *Composite structures*, 208, 566-573.
<https://doi.org/10.1016/j.compstruct.2018.10.057>
- Fajardo, J. I., Costa, J., Cruz, L. J., Paltán, C. A., & Santos, J. D. (2022). Micromechanical model for predicting the tensile properties of Guadua angustifolia fibers polypropylene-based composites. *Polymers*, 14(13), 2627.
<https://doi.org/10.3390/polym14132627>
- Fu, S. Y., Hu, X., & Yue, C. Y. (1998). A new model for the transverse modulus of unidirectional fiber composites. *Journal of Materials Science*, 33(20), 4953-4960.
<https://doi.org/10.1023/A:1004442520797>
- Gigante, V., Aliotta, L., Phuong, V. T., Coltelli, M. B., Cinelli, P., & Lazzeri, A. (2017). Effects of waviness on fiber-length distribution and interfacial shear strength of natural fibers reinforced composites. *Composites Science and Technology*, 152, 129-138.
<https://doi.org/10.1016/j.compscitech.2017.09.008>
- Gómez-Suárez, S. A., & Córdoba-Tuta, E. (2022). Materiales compuestos reforzados con fibras de fique-revisión. *Revista UIS Ingenierías*, 21(1), 163-178.
<https://doi.org/10.18273/revuin.v21n1-2022013>
- González-Estrada, O. A., Díaz-Ramírez, G., & Quiroga Méndez, J. E. (2018). Mechanical response and damage of woven composite materials reinforced with fique. *Key Engineering Materials*, 774, 143-148.
<https://doi.org/10.4028/www.scientific.net/KEM.774.143>
- Hajikarimi, P., & Sadat Hosseini, A. (2023). Analytical and Empirical Formulation. In *Constructional Viscoelastic Composite Materials: Theory and Application* (pp. 97-117). Singapore: Springer Nature Singapore.
https://doi.org/10.1007/978-981-99-1786-0_5
- Hiremath, V. S., Reddy, D. M., Mutra, R. R., Sanjeev, A., & Dhilipkumar, T. (2024). Thermal degradation and fire retardant behaviour of natural fibre reinforced polymeric composites-A comprehensive review. *Journal of Materials Research and Technology*, 30, 4053-4063.
<https://doi.org/10.1016/j.jmrt.2024.04.085>
- Jagadeesh, G. V., & Gangi Setti, S. (2020). A review on micro-mechanical methods for evaluation of mechanical behavior of particulate reinforced metal matrix composites. *Journal of Materials Science*, 55(23), 9848-9882.
<https://doi.org/10.1007/s10853-020-04715-2>
- Jasti, A., Chandra, B. A., & Biswas, S. (2023). Modified Halpin-Tsai model for predicting the mechanical properties of polymer composites reinforced with different cross-sectional fibers. *Materials Today: Proceedings*, 91, 14-18.
<https://doi.org/10.1016/j.matpr.2023.04.131>
- Laverde Sarmiento, V., Benjumea, J. M., & Rincón Ortiz, M. (2025). Chemical and Mechanical Characterization of Treated and Untreated Woven Figue Fiber Textiles as an Alternative External Reinforcement for Concrete. *Journal of Natural Fibers*, 22(1), 2462975.
<https://doi.org/10.1080/15440478.2025.2462975>
- Loos, M. (2014). *Carbon nanotube reinforced composites: CNT Polymer Science and Technology*. Elsevier.
<https://doi.org/10.1016/B978-1-4557-3195-4.00008-4>
- Miravete, A. (2020). *Materiales compuestos*. Volume 2. Reverté.
- Muñoz-Blandón, O., Ramírez-Carmona, M., Rendón-Castrillón, L., & Ocampo-López, C. (2023). Exploring the potential of fique fiber as a natural composite material: a comprehensive characterization study. *Polymers*, 15(12), 2712.
<https://doi.org/10.3390/polym15122712>
- Potluri, R., Diwakar, V., Venkatesh, K., & Reddy, B. S. (2018). Analytical model application for prediction of mechanical properties of natural fiber reinforced composites. *Materials Today: Proceedings*, 5(2), 5809-5818.
<https://doi.org/10.1016/j.matpr.2017.12.178>
- Raju, B., Hiremath, S. R., & Mahapatra, D. R. (2018). A review of micromechanics based models for effective elastic properties of reinforced polymer matrix composites. *Composite Structures*, 204, 607-619.
<https://doi.org/10.1016/j.compstruct.2018.07.125>

Sudheer, M., Pradyoth, K. R., & Somayaji, S. (2015). Analytical and numerical validation of epoxy/glass structural composites for elastic models. *American Journal of Materials Science*, 5(3C), 162-168.

<https://doi.org/10.5923/c.materials.201502.32>

Tham, M. W., Fazita, M. N., Abdul Khalil, H. P. S., Mahmud Zuhudi, N. Z., Jaafar, M., Rizal, S., & Haafiz, M. M. (2019). Tensile properties prediction of natural fibre composites using rule of mixtures: A review. *Journal of Reinforced Plastics and Composites*, 38(5), 211-248.

<https://doi.org/10.1177/0731684418813650>

Velásquez, S., Cardona, N., & Giraldo, D. (2018). Characterization of fique fibers and evaluation of mechanical properties, abrasive wear resistance, and processability of NR/SBR/BR-fique fibers composites. *Journal of Elastomers & Plastics*, 50(5), 435-447.

<https://doi.org/10.1177/0095244317731949>

Vignoli, L. L., Savi, M. A., Pacheco, P. M., & Kalamkarov, A. L. (2019). Comparative analysis of micromechanical models for the elastic composite laminae. *Composites Part B: Engineering*, 174, 106961.

<https://doi.org/10.1016/j.compositesb.2019.106961>

Wan, L., Ismail, Y., Sheng, Y., Ye, J., & Yang, D. (2023). A review on micromechanical modelling of progressive failure in unidirectional fibre-reinforced composites. *Composites Part C: Open Access*, 10, 100348.

<https://doi.org/10.1016/j.jcomc.2023.100348>

Wang, Y., & Huang, Z. (2017). A review of analytical micromechanics models on composite elastoplastic behaviour. *Procedia engineering*, 173, 1283-1290.

<https://doi.org/10.1016/j.proeng.2016.12.159>

Wang, Y., & Huang, Z. (2018). Analytical micromechanics models for elastoplastic behavior of long fibrous composites: A critical review and comparative study. *Materials*, 11(10), 1919.

<https://doi.org/10.3390/ma11101919>